iCHASM,
a flexible land-surface model that incorporates stable water isotopes.

M. J. Fischer[1]

[1]ANSTO, Institute for Nuclear Geophysiology, Menai, 2234, Australia

Address for correspondence
Dr M. Fischer
Australian Nuclear Science and Technology Organisation
Lucas Heights Science and Technology Centre
Private Mail Bag 1
Menai
NSW 2234
Australia
Email mjf@ansto.gov.au

Abstract

Isotope-enabled Global Climate Models (GCMs) have been previously used to investigate water isotope fluxes in present and past climate systems. Water isotope modelling is also important in modern ecosystem studies, for investigating the source and transport of moisture and carbon dioxide fluxes. However, in this modelling, there has only been limited investigation of the effect of parameterisation compexity on stable water isotope partitioning. The present study has two aims. The first is to incorporate a stable water isotope parameterisation into a flexible land surface scheme (LSS): the CHAmeleon Surface Model (CHASM). This scheme offers five different modes, each containing up to four water reservoirs (canopy interception, snowpack, root zone and bare ground storage), and each mode offers the opportunity to modify resistances to evaporative fluxes from these reservoirs. These different modes allow the effect of model complexity on different parameterisations to be explored within a common modelling framework. Two modelling experiments are reported which use the iPILPS Phase 1 forcing: the 'control' experiment and one using a simpler mode of CHASM comprising a bucket hydrology plus a fixed stomatal resistance. The additional set of experiments using iCHASM's variable modes shows, contrary to an earlier experiments with CHASM, that a land surface model with only a bucket hydrology scheme and constant surface resistance cannot reproduce the behaviour of an LSS that has additional functionality (such as bare ground evaporation, and canopy interception and aerodynamic, surface and stomatal resistances).

Keywords: Land surface model, GCM, stable isotopes, PILPS, iPILPS

1. Introduction

Land-surface modelling is a way of investigating how a land surface may partition the following components:

$$E(Pr) = E(Ro) + E(Evap) + E(\Delta S) \qquad (1)$$

$$E(Xnet) = E(Qle) + E(Qh) + E(Qg) \qquad (2)$$

Where *E*() is the expected value over some spatiotemporal scale, *Xnet* is net radiation W m^{-2}, *Qle* is latent heat in W m^{-2}, *Qh* is sensible heat in W m^{-2}, *Qg* is the sum of the heat flux into the snowpack, ground and canopy in W m^{-2}, *Pr* is precipitation in kg m^{-2}, *Evap* is total evapotranspiration in kg m^{-2}, and *Ro* is surface + subsurface run-off in kg m^{-2}, ΔS is the change in reservoir storage (e.g. canopy interception, snowpack, soil moisture) in kg m^{-2}. Complex land surface schemes have been developed in order to be incorporated in GCMs (Global Climate Models), and to use GCMs to make useful predictions about how climates may change in the future (e.g. Bagnoud *et al.* 2005), because land surface moisture and energy feedbacks directly affect climate. Isotope-enabled GCMs have also been developed, originally to investigate isotopes in the modern climate system and also to aid the interpretation of palaeo-isotope records (e.g. Jouzel *et al.* 1987). More recently, complex isotope-enabled land surface schemes have been developed to better understand ecosystem fluxes of moisture and carbon dioxide (Riley *et al.* 2002) because many ecosystem processes cause carbon and oxygen isotope fractionation. The isotopic-enabled land surface scheme described here was developed with all these points in mind. In equations 1 and 2, the terms on the right-hand side are a complex function of vegetation, soil and climate. An isotope-enabled land surface scheme also allows us to understand how the interaction between vegetation, soil and climate partitions the following components:

$$E(\delta Pr) = (E(Ro)E(\delta Ro) + E(Evap)E(\delta E) + E(\Delta S)E(\delta\Delta S))/E(Pr) \qquad (3)$$

This partitioning is independent of (1), due to the three additional independent unknowns (δRo, δE, $\delta\Delta S$) (so different LSSs may 'solve' the above equations differently: the solutions are non-unique). In this paper, the development of a water isotope parameterisation in a current land surface sheme (CHASM) is described. The new model (iCHASM) is tested using the iPILPS Phase 1 experiments (Henderson-Sellers *et al*., 2006), and the results of some additional experiments (that take advantage of iCHASM's flexible nature) are reported. These additional experiments examine how model complexity affects isotopic partitioning.

iCHASM is the first isotopically-enabled version of the land surface scheme (LSS) CHASM. The history of CHASM (the CHAmeleon Surface Model - a name given due to the multi-mode nature of the LSS by Desborough 1999) is tied closely to the history of PILPS. In the offline comparisons in Phase 1 and 2 of PILPS it was found that LSSs produce a wide range of behaviours (i.e., they partition the energy and moisture components, mentioned above, differently) when using the same atmospheric forcing and land surface parameters (e.g. Chen *et al*., 1997; Shao and Henderson-Sellers *et al*., 1996). Understanding the wide range of behaviours has been hindered by the large number of potential sources of these differences, the non-unique meaning of particular parameters in different schemes, and the complex interactions between these things. CHASM was developed as a scheme that has several modes, from a simple mode ('bucket' parameterisation, Manabe, 1969) to very complex modes (based on Deardoff, 1978 and Koster and Suarez, 1992). The advantage of this is that it allows general aspects of the surface energy balance parameterisation to be explored within a common modelling framework (Desborough, 1997; Desborough, 1999; Desborough *et al*., 2001). Thus, incorparating isotopes into CHASM allows us to also investigate the extent to which isotopic partitioning differences depend upon model complexity.

There are three sections to this paper. First, the modes of CHASM and its hydrology parameterisation are reviewed. Secondly, the new isotope parameterisation for CHASM is explained. Thirdly, the participation of iCHASM in the iPILPS Phase 1 experiments and some additional experiments (which take advantage of iCHASM's flexible modes), are discussed.

2. CHASM: Basic parameterisation

2.1 CHASM's modes

CHASM's modes have been documented by Desborough (1999), Pitman *et al*. (2003), and Bagnoud *et al*. (2005) and hence are only briefly summarised here. The modes are flexible in the sense that more than one tile can be used in any mode. Here, only one tile is used for all modes except SLAM (Simple Land-Atmosphere Mosaic).

In each mode, there are two optional water storage reservoirs (canopy and bare ground i.e. surface storage), and two compulsory reservoirs (root zone and snowpack i.e. if there is snow). Hydrologically, the root zone is a single layer of soil (that extends from the surface to typically 150 mm depth), with no sub-surface lateral flow or drainage (following the parameterisation of Manabe 1969).

Mode EB (Energy Balance) is the simplest mode of CHASM. There is no canopy or bare ground reservoir, so evaporation occurs from the rootzone and snow (if any) only. In this mode, the aerodynamic resistance can be calculated with or without a stability correction.

Mode RS is the same as EB, but with a surface resistance to snow-free evaporation. RS-I and RS-GI (modes 3 and 4) are the same as RS, but include canopy evaporation, and bare ground and canopy evaporation (with resistances), respectively.

In SLAM mode (the fifth mode), one tile contains bare ground and snow (if any), while the second tile contains only vegetation (subject to interception and transpiration). All types of evaporation have the full set of relevant resistances (e.g. aerodynamic, surface, stomatal).

Hence, CHASM's modes allow the LSS to run under a Manabe (1969) bucket configuration, with additional extras including explicit treatment of transpiration, bare ground evaporation and canopy interception (after Deardoff 1978), and a grouped mosaic structure with separate energy balances for each mosaic (Koster and Suarez 1992).

2.2 CHASM's hydrology

Each reservoir described above has a maximum capacity (except the snowpack, which has an infinite capacity). The maximum capacities were 150 mm (root zone), 40 mm (bare ground) and $0.1A^{[t]}a_v^{[t]}a_{leaf}^{[t]}$ (canopy interception, these terms are described below equation 4). Moisture can leave each reservoir only by evaporation (or transpiration in the case of the root zone), or from reservoir overflow.

The general equation for evaporation from a reservoir is:

$$E_x = A^{[t]}a_x^{[t]}\rho_a\beta_x^{[t]}(q^{*[t]} - q_a)/(r_a + r) \qquad \textit{(4)}$$

where x is the reservoir, $A^{[t]}$ is the fractional area of tile t, $a^{[t]}$ is the fractional area of the reservoir (or v, vegetation) on the surface of tile t, ρ_a is the density of water (kg m^{-3}), $\beta^{[t]}$ is the moisture availability index (may equal 1), $q^{*[t]}$ is the surface's saturated specific humidity (kg kg^{-1}), q_a is the specific humidity of the air (kg kg^{-1}), r_a is the aerodynamic resistance (s^{-1} m), and r is any additional resistances (s^{-1} m, may equal 0).

3. iCHASM: Isotope hydrology parameterisation

The isotope notation that is used here is as follows:

N = number of molecules of a certain compound in a certain reservoir

$R_{subscript}$ = isotope ratio of the subscript,

where the ratio is the heavy:light isotope ratio, e.g. $R_{reservoir} = (^{18}O:^{16}O)_{reservoir}$

The equilibration fractionation factor, α, can be defined in two ways (i.e. the isotopic fractionation factor of a phase change or chemical reaction can be defined as $\alpha = R_{product}/R_{reactant}$ or $\alpha = R_{product}/R_{reactant}$). Conventionally, $\alpha_{evap} = R_{reservoir}/R_{evaporate}$, so that $\alpha > 1$ (e.g. Gonfiantini 1986, Gat 1996). Also, $\varepsilon_{evap} = 10^3 ln(\alpha_{evap})$, and α and ε without an isotope designation means that the equations are relevant for either isotope (for example, α can be used for $\alpha^{18}O$ or α^2H). Note also that subscript t on any variable is a "point in time" reference.

Inputs and Overflow

For each reservoir, there are two possible ways of mixing the reservoir water with inputs. In a "total mixing" scheme:

$$RN(1+R)^{-1} = (R_1N_1)(1+R_1)^{-1} + (R_2N_2)(1+R_2)^{-1} \qquad (5)$$

where, $R = R_{reservoir(t)}$, note that the reservoir contains a total of N molecules of which $N(1+R)^{-1}$ molecules are the abundant isotope species, and $RN(1+R)^{-1}$ molecules are the rare isotopic species.

$R_1 = R_{reservoir(t-1)}$,

$R_2 = R_{inputs}$ = weighted isotope ratio of any inputs

$R_{overflow(t)} = R_{reservoir(t)},$

$N = N_1 + N_2$

N_1 = number of molecules of water in reservoir, N_2 = number of molecules of input water of input water

In a "partial mixing" scheme:

$$RN(1+R)^{-1} = (R_1N_1)(1+R_1)^{-1} + (R_2N_2)(1+R_2)^{-1} \qquad (6)$$

$R_{overflow(t)} = R_{inputs(t)}$

$N = N_1 + N_2$

$N \leq N_1MAX$

N_1MAX is the maximum storage capacity of the reservoir.

In iCHASM, the canopy interception and snowpack use a total mixing sheme, while the bare ground and rootzone use a partial mixing scheme. The effect of these different mixing schemes on land surface isotopic fluxes could be further investigated by sensitivity testing.

Evaporation and Transpiration

The isotope ratio of the residual water in a reservoir, and the evaporation and transpiration flux are as follows:

Residual water in a reservoir after evaporation:

$$R_{reservoir} = R_0 f^{(1/\alpha_{evap})-1} \qquad (7)$$

where,

R_0 = initial isotope ratio in the reservoir

f = fraction of water remaining in the reservoir after an evaporation event

α_{evap} is explained above, the Craig-Gordon solution to this term is outlined below

The evaporation flux:

$$R_{evap} = \frac{R_0(1 - f^{\alpha_{evap}})}{(1 - f)} \qquad (8)$$

The transpiration flux:

$$R_{Tr} = \mathrm{R}_{rootzone} = R_{xylem} \qquad (9)$$

The tranpiration flux is assumed to be in steady-state with the rootzone water, with respect to its isotopic composition (see Gat 1996). That is, the vegetation (transpiration) is assumed to be non-fractionating (as in GISS, ECHAMiso and REMOiso) (these are isotope-enabled models belonging to Goddard Institute of Space Sciences, GISS and the European Centre HAMburg, ECHAM; REMOiso is a REgional MOdel nested in ECHAMiso) (Jouzel, 1987; Hoffmann *et al*., 1998; Sturm *et al*., 2005). A non steady-state transpiration isotope parameterisation may be incorporated into iCHASM in the future.

Solution to α_{evap}:

The Craig-Gordon (1965) solution to α_{evap} (added to by Gonfiantini 1986 and Cappa *et al.*, 2003) is as follows:

$$\alpha_{evap} = \frac{1-h}{\alpha_{kin}{}^{-1}(\alpha_{eq}{}^{-1} - hR_{atm} / R_{reservoir})} \qquad (10)$$

$$\Delta\varepsilon^{18}O = 28.4n(1\text{-}h)‰ \qquad (11)$$

$$\Delta\varepsilon^{2}H = 25.0n(1\text{-}h)‰$$

$$ln(\alpha_{kin}) = 10^{-3}\Delta\varepsilon$$

$$\varepsilon^{18}O = 1137(T_k)^{-2} - 0.4156(T_k)^{-1} - 0.00207 \qquad (12)$$

$$\varepsilon^{2}H = 24844(T_k)^{-2} - 76.248(T_k)^{-1} + 0.05261$$

$$ln(\alpha_{eq}) = 10^{-3}\varepsilon$$

(alternatively, see Horita and Wesolowski 1994)

T_k = Temperature in Kelvin

h = relative humidity (as a ratio)

n = turbulence parameter. This is reservoir dependent. Soil n = 1, leaf n = 1, free-standing water n = 0.5. This is due to the type of air layer that a reservoir is evaporating into. For water evaporating into an air layer that is stagnant or turbulent, n is ~1 or ~0.5 respectively (see Gat 1996 for further explanation) .

α and ε were explained at the start of this section.

4. Description and Results of Experiments

iCHASM participated in the initial iPILPS experiments as documented in Henderson-Sellers *et al.*, 2006.

Time-invariant surface properties and LSS initialisation

iCHASM was initialised and run using the initial values (e.g. for surface temperature and the isotope ratio of the water reservoirs) and time-invariant surface properties (such as leaf are index, and the fraction of vegetation on the surface) as set by the iPILPS Phase 1 experiment (Henderson-Sellers *et al.*, 2006). Additional parameters which were required by iCHASM (and not specified by iPILPS) included snow, vegetation and ground roughness lengths, the vegetation and snow albedos (see Table 1), and the depth of layers for soil temperature calculations (0-5, 5-15, 15-50, 50-100 cm and 1-2 m).

EQY1, using iCHASM's different modes

In the EQY1 experiments, iCHASM reached equilibrium (as defined in Henderson-Sellers *et al*., 2006) in 4-5 model years (for Manaus, Munich and Tumbarumba). The bulk moisture and energy conservation budgets of all participating ILSSs are discussed in Henderson-Sellers *et al*., 2006. (iCHASM has good energy and moisture conservation; the isotopic conservation is discussed further below). The focus here is on isotopic partitioning (in iCHASM) and its sensitivity to iCHASM's different modes.

An example of iCHASM output (using mode RS-GI, and Tumbarumba as the location) for the equilibrium year is displayed in Figures 1 and 2. The annual cycle of the two soil reservoirs in RS-GI (bare ground and rootzone) are displayed in Figures 2b and 2c, respectively. The bare ground reservoir (*Soil1*) is characterised by larger isotopic fluctuations then the rootzone (*Soil2*), since the bare ground has a smaller maximum capacity, and hence dries out more quickly (causing isotopic enrichment), especially during the summer months in Tumbarumba. The enrichment is periodically halted by isotopically depleted rainfall events. During the winter months, when temperatures are colder, and relative humidity higher, water in the soil reservoirs (especially bare ground) maintains a value that is much closer to the weighted isotope ratio of the precipitation. This is clearly seen in Figure 2, where the hourly weighted averages over a month properly show the relationship between the precipitation and soil reservoirs. In Figure 2, the weighted isotope ratio of the bare ground reservoir is close to the weighted isotope ratio of the precipitation for July, but very different for January. The root zone water is enriched compared with the precipitation in July, presumably due to the enrichment that occurred during the previous season: the residence time of water in the rootzone is greater than that of the bare ground. Further, the root zone in winter does not respond (as much as in summer) to isotopically depeleted rainfall events, because the reservoir is near full (there is less evaporation in winter) and the rainfall is partitioned more into run-off than into infiltration. Similar patterns are found in the annual and daily isotopic plots from Munich and Manaus (not shown here), that is, the patterns are dependent upon the interplay between reservoir size, evapotranspiration amount, and the amount, isotopic characteristics, and average recurrence interval of the rainfall.

Figures 3 and 4 show $\delta^2H/\delta^{18}O$ plots over two different timescales (seasonal and diurnal) for iCHASM's RS-GI mode. The symbols in these plots correspond to the following fluxes or reservoirs: A = *Ro* (run-off), B = *Tr* (transpiration), C = *Ev* (soil evaporation), D = *Soil1* (bare ground moisture), E = *Soil2* (rootzone moisture). In the monthly $\delta^2H/\delta^{18}O$ plots, the 12 points for each flux/reservoir corresponds to the 12 months. On the monthly timescale, run-off (A) generally lies along the GMWL (Global Meteoric Water Line), and has an isotope ratio which is similar to the monthly rainfall. The residual soil waters (D&E) lie along an evaporation line, with the corresponding evaporate (C) in the isotopically-depleted quadrant. The canopy interception evaporation flux is also found in the same quadrant (the canopy interception and evaporation flux are not shown, to simplify the figures). The transpiration (B) also lies along the same evaporation line, because for steady-state non-fractionating vegetation, the transpiration = rootzone water (Gat 1996). The plots from the three locations show similar trends, but otherwise are not particularly informative.

The daily $\delta^2H/\delta^{18}O$ plots (Figure 4), though, show additional features. Firstly, there is a change in the relationship of B, D and E from summer to winter (seen most clearly for the locations Manaus and Tumbarumba). B and E are always similar due to the steady-state non-fractionating vegetation. The displacement of D (bare ground reservoir) from E (rootzone), however, depends upon the antecedent water in the root zone (from the previous season) and the relative humidity of the air in the current season. Note that the slope of the evaporation line extending from A (intersecting the GMWL) to D and E is largely dependent on the relative humidity in different seasons. In the austral summer (January), for Tumbarumba, both D and E are isotopically enriched and lie along an evaporation line, characterised by a slope less than 8 (Gat 1996). In the austral winter, both D and E move back onto the GMWL, because there is less evaporation, and also some input from rainfall (isotopic rainout during precipitation occurs mainly under equilibrium conditions, and hence precipitation falls on the GMWL). However, D and E are separated on the GWML during winter because the rootzone reservoir (E) is larger than the bare soil reservoir (D) and not replenished by recent rainfall to the same extent (for reasons discussed above). In Manaus, a different pattern is found. D and E lie along an evporation line in July, and along the GMWL in January (January is more humid than July). However, D and E both lie close to A (in this case δRo approximates δPr), due to large amounts of isotopically depleted rainfall and relatively fast residence time of moisture through the rootzone, due to large transpiration fluxes. Thus, isotopes in land surface schemes should be useful for assessing how different components of the soil reservoir (such as bareground and root zone) need to be parameterised in order to achieve adequate moisture partitioning in a land surface scheme. The different components that are shown to be important by the examples here include the size of the reservoir, the proportion of each reservoir used for transpiration and how the different soil layers are hydrologically connected.

Additional sensitivity experiments were performed using CHASM's RS mode, to investigate whether a Manabe bucket LSS containing a constant surface resistance term could have the same functionality as an LSS containing additional complexity.

These experiments were thus similar to those found in Section 4 in Desborough (1999). The experimental results are shown in Figure 5. The numbers 1-4 correspond to CHASM's modes EB (1) and RS (2-4) (The X's in this Figure are described below). In the RS mode, a constant surface resistance was added with values of 50, 75 and 100 s m^{-1}. Figure 5a shows a similar behaviour to that observed by Desborough (1999): adding the constant surface resistance makes iCHASM behave like a more complex LSS in terms of the partitioning of available energy into latent and sensible heat. (In Figure 5a, bucket-type schemes are found to the lower right on each net radiation line, while Soil-Vegetation-Atmosphere Transfer models - using parameterisations developed in the 1980's - are found to the upper left. The X's show the land surface schemes that participated in the iPILPS Phase 1 experiment. These schemes cover a range of complexities, see Henderson-Sellers *et al.*, 2006. The X's fall slightly away from the mean net radiation lines because each scheme has a slightly different mean annual net radiation, and the points are not scaled for this, in order to keep the points separated for clarity). Figure 5b shows the corresponding iPILPS plot (explained in Henderson-Sellers *et al.*, 2006). (Note that the isotopic balance of iCHASM's modes EB and RS is proven in this diagram). In this plot, in the RS modes, the evaporation fluxes have become isotopically enriched while the run-off is isotopically depleted. This moves the iCHASM simulations down the slope relative to the other ILSSs. The explanation, here, is that under higher constant surface resistance, there is less evapotranspiration, but the ratio of transpiration to total evapotranspiration becomes greater, and the isotopic flux of transpiration is approximately = δrootzone. Hence, the addition of a constant surface resistance does not make iCHASM partition the isotopic budget in a way that is similar to a more complex ILSS.

CHASM and iCHASM

Through experiments with CHASM, Desborough (1999) drew two main conclusions:

i) Firstly, for the simulation of latent heat in LSSs on an annual timescale, a bucket LSS containing a constant surface resistance term could have the same functionality as an LSS containing additional complexity (such as bare-ground evaporation, and canopy interception and evaporation resistances).

ii) Secondly, for the simulation of latent heat in LSSs on a diurnal timescale, a bucket LSS containing a constant surface resistance term does not have the same functionality as a LSS containing additional complexity (such as bare-ground evaporation, and canopy interception and evaporation resistances). That is, additional scheme complexity (beyond a constant surface resistance term) is required to make a bucket LSS behave like a more complex LSS.

In the new experiments with iCHASM shown here, the new conclusion is that:
A bucket LSS with a constant surface resistance cannot mimic a more complex LSS, even on an annual timescale. This contrasts with conclusion i) above. While there is a decrease in total evaporation in the iCHASM RS runs (as in a more complex LSS), there is isotopic enrichment in the total evapotranspiration flux, due to change in the tranpiration/evapotranspiration ratio. This is not observed in a typical PILPS plot (e.g. Figure 5a), which Desborough (1999) used as a test for assessing point I) above.

Further experiments are necessary to determine the processes that must be included in an LSS to adequately simulate *both* the energy and isotopic budget. The conclusions drawn here show the value of isotopes in LSSs in understanding how land surfaces partition energy, moisture and the isotopes in terrestrial moisture. Although this paper suggests that it is not useful to use the simple modes of iCHASM (or equivalent schemes) in an isotopically-enabled GCM, it will be necessary and valuable to run further experiments with the complex modes of iCHASM (RS-GI and SLAM), in order to determine the processes that must be included in an ILSS to adequately simulate the energy, moisture and isotopic partioning.

5. Summary and Conclusions

A stable water isotope parameterisation has been added to a flexible land surface model, CHASM, allowing modelling experiments to be conducted which use the isotopes to investigate how a land surface simultaneously partitions energy and moisture components. $\delta^2H/\delta^{18}O$ plots at two different timescales (seasonal and diurnal) show the influence that the reservoir residence time, the humidity of the season, the tranpiration amounts and the stochastic properties of the precipitation, have on the isotope partitioning in the bare ground and root zone reservoirs. The results illustrate the value of isotopes in land surface schemes for assessing how different components of the soil reservoir need to be parameterised in order to achieve adequate moisture partitioning overall.

An earlier set of experiments using CHASM (Desborough 1999) concluded that the ability of an LSS to adequately predict latent heat and evaporation at monthly timescales required no more surface energy balance complexity than a constant surface resistance. The additional set of experiments reported here (over and above those with iCHASM reported in Henderson-Sellers *et al.,* 2006) shows that although the addition of a constant surface resistance to a bucket scheme may lead to adequate latent heat and total evaporative fluxes, this level of simplicity fails to replicate the isotopic partitioning of a more complex LSS. This is because the surface resistance does not affect properties such as the reservoir residence time and the transpiration/evpotranspiration ratio, in the correct direction. Future experiments with iCHASM will address wider issues including model sensitivity, and how geographic variation and land-atmosphere feedbacks affect the ability of ILSSs to properly partition the energy, moisture and isotopic fluxes.

Acknowledgments

I am grateful to Professor Andy Pitman for allowing me to incorporate isotopes into CHASM in this study, and to the anonymous reviewers whose comments have improved this paper.

References

Bagnoud, N., Pitman, A. J., McAveney, B. J. and Holbrook, N. J., 2005. The contribution of the land surface energy balance complexity to differences in means, variances and extremes using the AMIP-II methodology. *Climate Dynamics*, 25, 171-188.

Cappa, C. D., Hendricks, M. B., DePaolo, D. J. and Cohen, R.C., 2003. Isotopic fractionation of water during evaporation. *Journal of Geophysical Research*, 108, 4525-4534.

Chen T.H., Henderson-Sellers, A., Milly, P.C.D., Pitman, A.J., Beljaars, A.C.M., Polcher, J., Abramopoulos, F., Boone, A., Chang, S., Chen, F., Dai, Y., Desborough, C.E., Dickinson, R.E., Dumenil, L., Ek, M., Garratt, J.R., Gedney, N., Gusev, Y.M., Kim, J., Koster, R., Kowalczyk, E.A., Laval, K., Lean, J., Lettenmaier, D., Liang, X., Mahfouf, J.-F., Megelkamp, H.-T., Mitchell, K., Nasonova, O.N., Noilhan, J., Robock, A., Rozensweig, C., Schaake, J., Schlosser, A., Schulz, J.P., Shao, Y., Shmakin, A.B., Verseghy, D.L., Wetzel, P., Wood, E.F., Xue, Y., Yang, Z.-L. and Zeng, Q., 1997. Cabauw experimental results from the Project for Intercomparison of Land-surface Parameterization Schemes. *J. Climate,* 10**,** 1194-1215.

Craig, H. and Gordon, L. I., 1965. Deuterium and oxygen 18 variations in the ocean and marine atmosphere. In: Tongiorgi, E. (Ed.), *Stable Isotopes in Oceanographic Studies and Paleotemperatures*. Lab. Geologia Nucleare, Pisa, Italy, pp. 9-130.

Deardoff, J. W., 1978. Efficient prediction of ground surface temperature and moisture, with inclusion of a layer of vegetation. *Journal of Geophysical Research*, 83, 1889-1903.

Desborough, C. E., 1997. Evaporative surface stress in land surface models: impact of inter-model parameterisation differences. PhD Thesis, Macquarie University, 136 pp.

Desborough, C. E., 1999. Surface energy balance complexity in GCM land surface models. *Climate Dynamics*, 15, 389-403.

Desborough, C. E., Pitman, A. J. and McAveney, B. J., 2001. Surface energy balance complexity in GCM land surface models, Part II: coupled simulations. *Climate Dynamics*, 17, 615-626

Gat, J. R., 1996. Oxygen and hydrogen isotopes in the hydrologic cycle. *Annual Review of Earth and Planetary Sciences*, 24, 225-262.

Gonfiantini, R., 1986. Environmental isotopes in lake studies. In: Fritz, P. and Fontes, J. C. (Eds.), *Handbook of Environmental Isotope Geochemistry (Volume 3)*. Elsevier, New York, pp. 113-168.

Henderson-Sellers, A., Fischer, M. J., Aleinov, I., McGuffie, K., Riley, W. J., Schmidt, G. A., Sturm1, K., Yoshimura, K and Irannejad, P., 2006. Stable water isotope simulation by current land-surface schemes: results of iPILPS Phase 1. *Global and Planetary Change*, in press.

Hoffmann, G., Werner, M., and Heimann, M. 1998. The water isotope module of the ECHAM atmospheric general circulation model - A study on time scales from days to several years. *Journal of Geophysical Research*, 103, 16871-16896.

Horita, J. and Wesolowski, D. J., 1994. Liquid-vapor fractionation of oxygen and hydrogen isotopes of water from the freezing to the critical temperature, *Geochimica et Cosmochimica Acta,* 58, 3425-3437.

Jouzel, J., Russell, G. L., Suozzo, R. J., Koster, R. D., White, J. W. C., and Broecker, W. S. 1987. Simulations of HDO and $H_2{}^{18}O$ atmospheric cycles using the NASA GISS general circulation model: the seasonal cycle for present-day conditions. *Journal of Geophysical Research*, 92, 14739-14760.

Koster, R. D. and Suarez, M. J., 1992. Modelling the land surface boundary in climate models as a composite of independent vegetation stands. *Journal of Geophysical Research*, 97, 2697-2715.

Manabe, S., 1969. Climate and ocean circulation: 1, the atmospheric circulation and the hydrology of the Earth's surface. *Monthly Weather Review*, 97, 739-805.

Pitman, A. J., Xia, Y., Leplastrier, M. and Henderson-Sellers, A., 2003. The CHAmeleon Surface Model: description and use with the PILPS phase 2(e) forcing data. *Global and Planetary Change*, 38, 121-135.

Riley, W. J., Still, C. J., Torn, M. S. and Berry, J. A, 2002. A mechanistic model of $H_2{}^{18}O$ and $C^{18}OO$ fluxes between ecosystems and the atmosphere: Model description and sensitivity analyses. *Global Biogeochemical Cycles*, 16, doi:10.1029/2002GB001878.

Shao, Y., and Henderson-Sellers, A. 1996. Validation of soil moisture simulation in land surface parameterisation schemes with HAPEX data. *Global and Planetary Change*, 13, 11-46.

Sturm, K., Hoffmann, G., Langmann, B. and Stichler, W., 2005. Stable water isotopes in precipitation: a regional circulation modelling approach. *Hydrological Processes*, 19, 3425-3444, doi: 10.1002/hyp.5979.

Tables

Surface property	Value
Roughness length, bare soil	0.01 m
Roughness length, vegetation	0.1 m
Roughness length, snow	0.00024 m
Albedo, vegetation	0.15
Albedo, snow (initial)	0.75
Depth, bare soil	0.04 m
Depth, rootzone	0.15 m
Minimum canopy resistance	40 s m^{-1}

Table 1: Land surface properties used in iCHASM and not defined by iPILPS Phase 1 experiments

Figure captions

Figure 1: Various components of the annual water isotope budget (here all δs refer to $\delta^{18}O$). (a) δPr = isotope ratio of total precipitation, (b) $\delta Soil1$ = isotope ratio of bare ground, (c) $\delta Soil2$ = isotope ratio of the root zone, all relative to VSMOW for the final year of the equilibration simulation, EQY1, for Tumbarumba.

Figure 2: Various components of the diurnal water isotope budget (here all δs refer to $\delta^{18}O$) for the final year of the equilibration simulation, EQY1, for Tumbarumba for (a) January, and (b) July. All δs are relative to VSMOW.

Figure 3: Components of the twelve monthly water isotope cycle, shown as a $\delta^{18}O$:$\delta^{2}H$ plot, for (a) Manaus, (b) Munich, (c) Tumbarumba. A = δRo = isotope ratio of run-off, B = δTr = isotope ratio of transpiration, C = δEv = isotope ratio of soil evaporation, D = $\delta Soil1$ = isotope ratio of bare ground, E = $\delta Soil2$ = isotope ratio of soil reservoir; all relative to VSMOW for the final year of the equilibration simulation, EQY1. The GMWL line is the solid diagonal line.

Figure 4: Components of the 24 hourly water isotope cycle, for January and July, shown as a $\delta^{18}O$:$\delta^{2}H$ plot, for (a-b) Manaus, (c-d) Munich, (e-f) Tumbarumba. A = δRo = isotope ratio of run-off, B = δTr = isotope ratio of transpiration, C = δEv isotope ratio of soil evaporation, D = $\delta Soil1$ = isotope ratio of bare ground, E = $\delta Soil2$ = isotope ratio of soil reservoir; all relative to VSMOW for the final year of the equilibration simulation, EQY1. The GMWL line is the solid diagonal line.

Figure 5: Components of the annual mean (a) energy budget and b) isoflux budget (averaged over the year), for iCHASM (numbers) and anonymous models participating in iPILPS (X). iCHASM's different RS modes are designated by number: 1 = EB, 2 = RS (surface resistance, $r_s = 50\ s\ m^{-1}$), 3 = RS ($r_s = 75\ s\ m^{-1}$), 4 = RS ($r_s = 100\ s\ m^{-1}$). Locations are designated by line type (Manaus = dashed, Munich = dotted, Tumbarumba = solid line).

Figures:

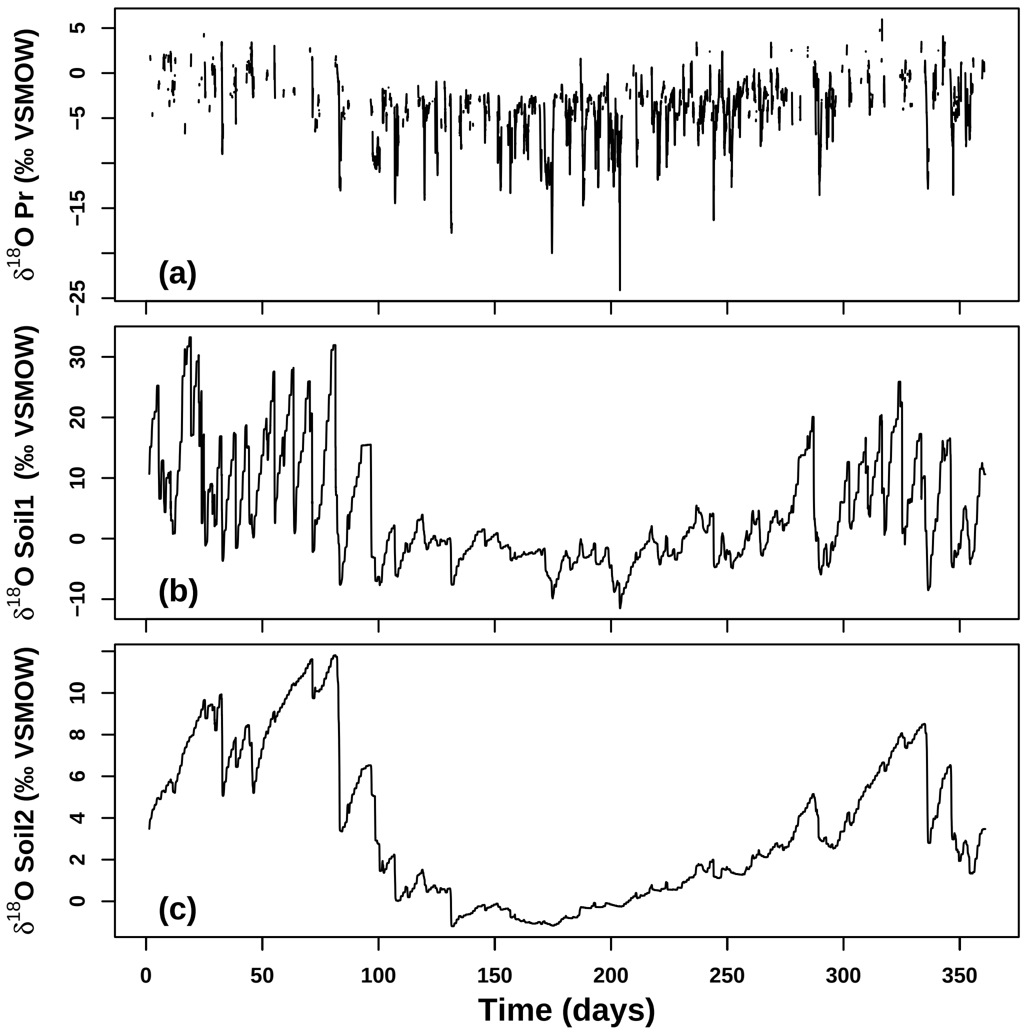

Figure 1

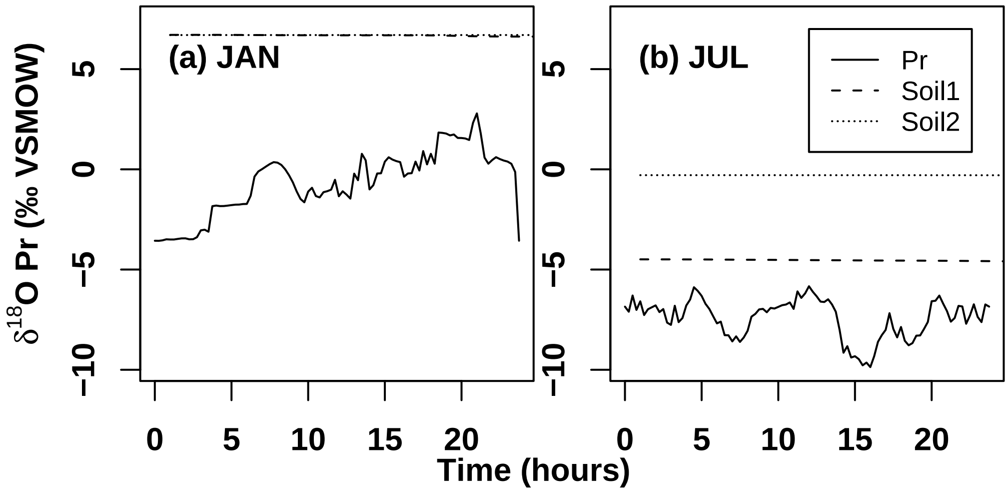

(a) JAN
(b) JUL
Pr
Soil1
Soil2
δ18O Pr (‰ VSMOW)
5
0
−5
−10
0
5
10
15
20
Time (hours)

Figure 2

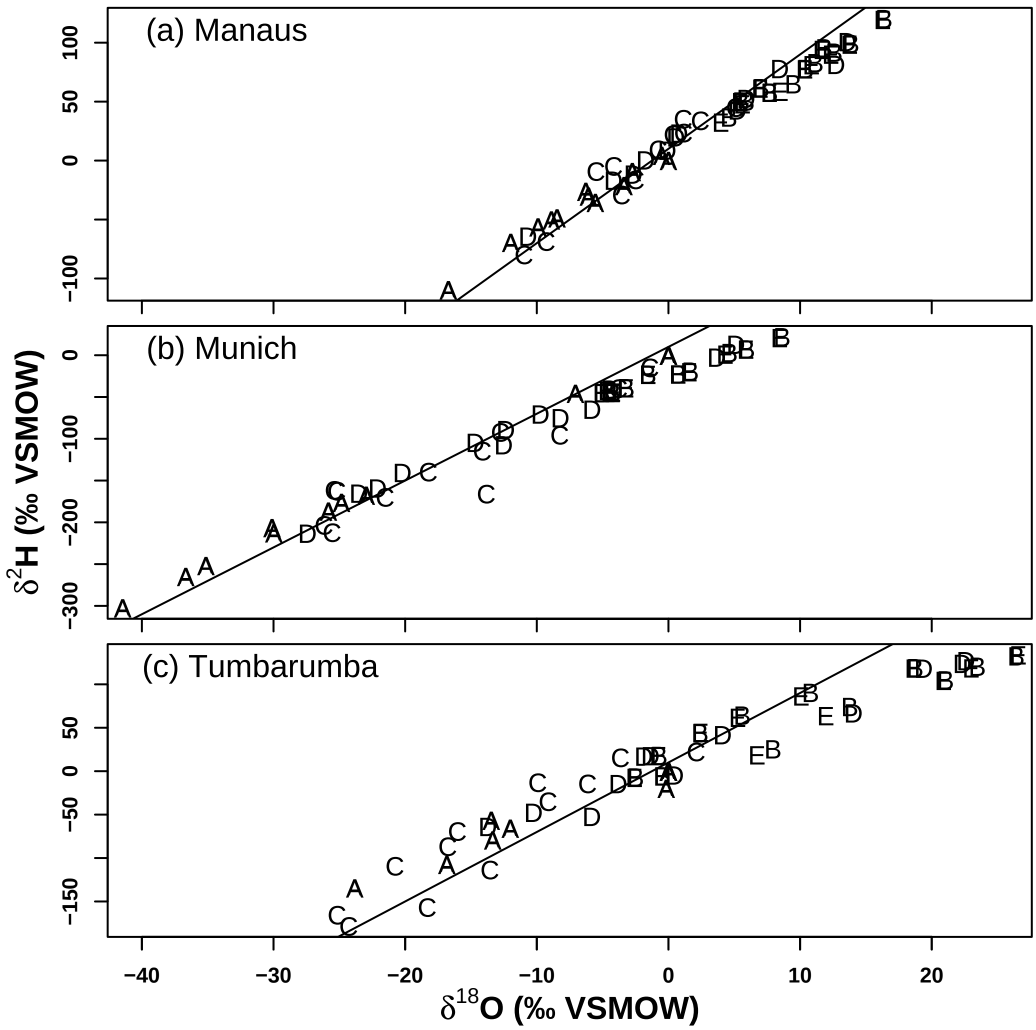
(a) Manaus
(b) Munich
(c) Tumbarumba
δ^2H (‰ VSMOW)
δ^{18}O (‰ VSMOW)

Figure 3

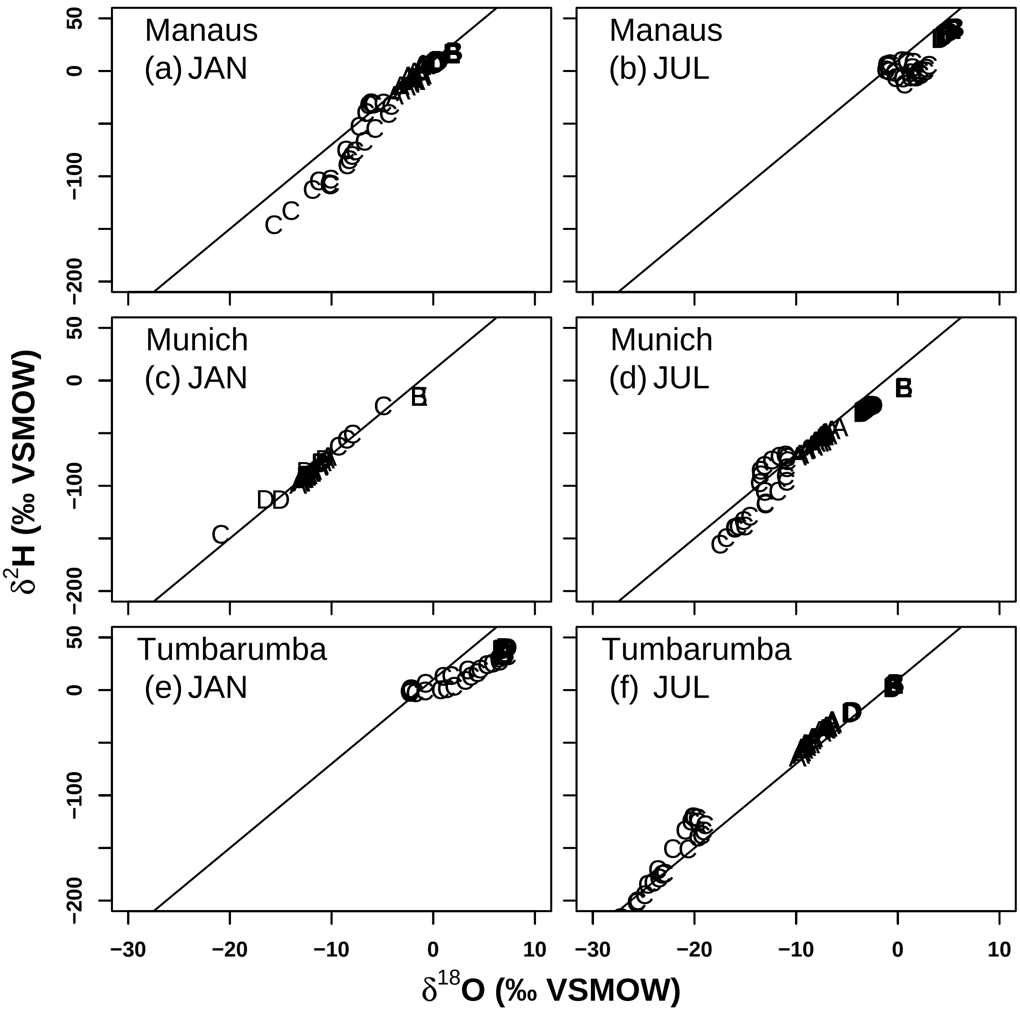
Manaus
(a) JAN
Manaus
(b) JUL
Munich
(c) JAN
Munich
(d) JUL
Tumbarumba
(e) JAN
Tumbarumba
(f) JUL
δ2H (‰ VSMOW)
δ18O (‰ VSMOW)
50
0
−100
−200
−30
−20
−10
0
10

Figure 4

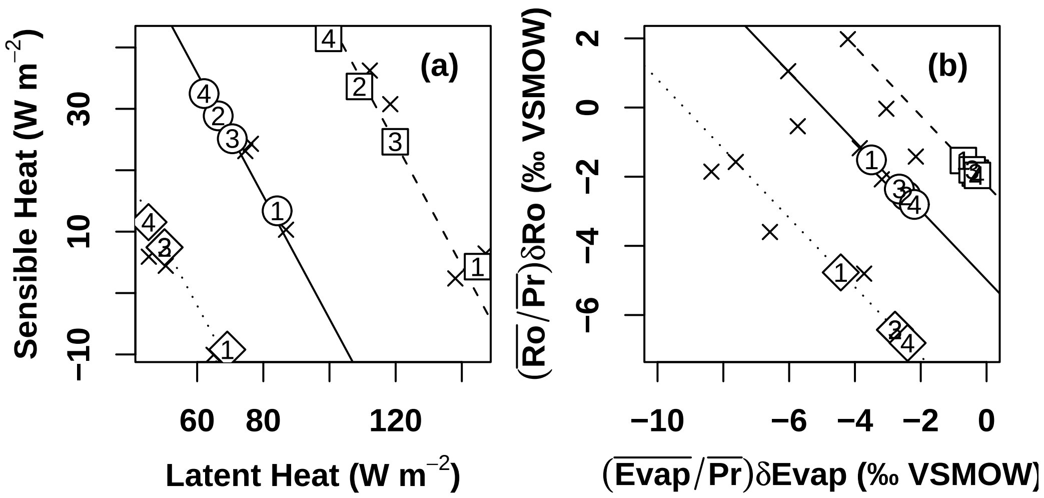
(a)
Sensible Heat (W m^{-2})
Latent Heat (W m^{-2})
−10
10
30
60
80
120
(b)
$(\overline{Ro}/\overline{Pr})\delta Ro$ (‰ VSMOW)
$(\overline{Evap}/\overline{Pr})\delta Evap$ (‰ VSMOW)
2
0
−2
−4
−6
−10
−6
−4
−2
0

Figure 5